

Microbial Communities Collectively Recycle Cadavers Over One Year of Human Decomposition

Allison R. Mason¹, Lois S. Taylor², Naomi E. Gilbert¹,
Steven W. Wilhelm¹, Jennifer M. DeBruyn^{1,2*}

¹Department of Microbiology, University of Tennessee-Knoxville, 1311
Cumberland Avenue, Knoxville, 37996.

²Department of Biosystems Engineering and Soil Science, University of
Tennessee-Knoxville, 2506 E.J. Chapman Drive, Knoxville, 37996.

*Corresponding author(s). E-mail(s): jdebruyn@utk.edu;

Abstract

Background During terrestrial vertebrate decomposition, host and environmental microbial communities work together to drive biogeochemical cycling of carbon and nutrients. These mixed communities undergo dramatic restructuring in the resulting decomposition hotspots. To reveal the succession of both the active microbial members and the metabolic pathways they use, we generated metatranscriptomes from soil samples collected over one year from below three decomposing human bodies.

Results Soil microbes increased expression of heat shock proteins in response to decomposition products changing physiochemical conditions (*i.e.*, reduced oxygen, high salt). Increased fungal lipase expression implicated fungi as key decomposers of fat tissue. Expression of nitrogen cycling genes was phased with soil oxygen concentrations: during hypoxic soil conditions, genes catalyzing N-reducing processes (*e.g.*, hydroxylamine to nitric oxide and nitrous oxide to nitrogen gas during reduced oxygen conditions) were increased, followed by increased expression of nitrification genes once oxygen diffused back into the

047 soil. Increased expression of bile salt hydrolases implicated a microbial source
048 for the high concentrations of taurine typically observed during vertebrate
049 decomposition.

050 **Conclusions** Collectively, microbial gene expression profiles remained altered
051 even after one year. Together, we show how human decomposition alters soil
052 microbial gene expression, revealing both ephemeral and lasting effects on soil
053 microbial communities.
054

055 **Keywords:** Human Decomposition, Microbial Succession, Metatranscriptomics, Soil
056 Microbial Ecology
057
058
059
060
061

062 Introduction 063

064
065 Soil microbial communities are important drivers of ecosystem processes in terrestrial
066 environments. Many soil microbes are decomposers that degrade complex organic mat-
067 ter and drive nutrient cycling in terrestrial ecosystems. Environmental disturbances
068 can impact the presence and/or activity of soil microorganisms involved in these
069 cycles, ultimately affecting nutrient availability and greenhouse gas emissions, such as
070 CO₂ and N₂O [1, 2]. Vertebrate death and subsequent carcass deposition in terrestrial
071 ecosystems is one disturbance resulting in the deposition of large quantities of organic
072 C and N [3–10], along with other elements (P, K, S, *etc.*) [11], which collectively
073 stimulate microbially-mediated biogeochemical cycling. In addition to this, changes
074 in pH, temperature, and fluctuations in soil oxygen provide abiotic filtering further
075 impacting microbial metabolic strategies [7–9, 11–13]. Vertebrate decomposition also
076 results in mixing of host and environmental microbes: the animal’s microflora are
077 flushed into the soil along with decomposition products where they further contribute
078 to decomposition processes (*e.g.*, organic nitrogen mineralization) [14].
079
080
081
082
083
084
085
086
087
088

089 While C and N transformations have been documented during decomposition, the
090 functional response of microbes and their roles in nutrient cycles remain unclear. The
091
092

composition and structure of decomposition-impacted soil microbial communities have
 been investigated using sequencing of marker genes amplicons (*i.e.*, 16S rRNA, 18S
 rRNA, ITS). This has allowed for the identification of changes in microbial biodi-
 versity and taxonomic succession in response to vertebrate decomposition, revealing
 patterns that include increases in the anaerobic taxa *Firmicutes* and *Bacteroidetes*
 [15]. However, few studies have integrated soil biogeochemistry with microbial com-
 munity composition, which can further help to describe microbial ecology in these
 decomposition systems. Taylor et al. (2024) [13] showed that fungal community shifts
 were linked to changes in soil dissolved oxygen, highlighting interactions between soil
 microbes and changes in the surrounding environment. While insightful for making
 potential connections between taxa and environment, these analyses do not inform
 which taxa are active members of the community, which functional pathways/genes
 are expressed, and how these pathways facilitate decomposition processes.

RNA sequencing (*i.e.*, metatranscriptomics) and metabolomics can be used to inves-
 tigate microbial community functional succession during decomposition. They can
 identify how ecological functions, including C and N cycling, are impacted by decom-
 position events in terrestrial ecosystems. To date, applications of metatranscriptomics
 to vertebrate decomposition samples have been limited to internal host communities
 [16, 17]: Burcham et al. (2019) [16] revealed differential expression of amino acid
 and carbohydrate metabolism in the heart during mouse decomposition, while Ashe
 et al. (2021) [17] documented taxonomic shifts in gene expression of oral microbial
 communities during human decomposition.

We expected that the impacted soil microbial community, which includes a mix of host
 and environmental taxa, would also have altered gene expression profiles, given the
 release of decomposition byproducts into the soil during terrestrial decomposition. We
 previously assessed the decomposition-impacted soil metabolome [18], demonstrating a

139 prevalence of amino acids and suggesting upregulation of organic nitrogen metabolic
 140 pathways. Additionally, DeBruyn et al. (2021) [18] showed the soil metabolome was
 141 surprisingly still altered compared to starting conditions at the end of that 21-week
 142 study, suggesting long-term impacts of decomposition on soil microbial functioning.
 143
 144 Here, we investigated soil microbial gene expression during a one-year period of human
 145 decomposition. The overarching goal of this work was to assess the effects of vertebrate
 146 decomposition on ecosystem function by characterizing community-level shifts in soil
 147 microbial function. We hypothesized that: (i) gene expression would shift over time as
 148 resources were consumed and transformed and soil chemical and physical conditions
 149 changed due to the influx of decomposition products during soft tissue degradation
 150 [8, 9, 18]; (ii) gene expression for enzymes involved in nitrogen cycling would be altered,
 151 as changes in nitrogen pools have been previously described in decomposition soils [8];
 152 (iii) expression of genes involved in lipid metabolism would increase, as lipids from
 153 the body entered the soil during decomposition and previous studies identified lipoly-
 154 tic organisms in decomposition soils [12, 19]; (iv) microbial expression profiles in the
 155 impacted soil would not fully recover and remain altered even after a year, as previ-
 156 ous studies have shown that community composition was still altered at least a year
 157 after decomposition began [20, 21]. We analyzed metatranscriptomes of soil samples
 158 collected at six key timepoints over one year of human decomposition to determine
 159 the identity of active populations and the expression of genes and pathways relevant
 160 to the enhanced biogeochemical cycling observed in decomposition hotspots. We com-
 161 pared gene expression between decomposition timepoints and control soils that were
 162 unexposed to decomposition products to identify functions or functional pathways
 163 of interest. We show: (i) decomposition shifts soil microbial community gene expres-
 164 sion, with the effects still measurable after one year; (ii) expression of genes related to
 165 stress response are elevated in decomposition soils; (iii) expression of genes encoding
 166
 167
 168
 169
 170
 171
 172
 173
 174
 175
 176
 177
 178
 179
 180
 181
 182
 183
 184

triacylglycerol lipase differed between fungi (increased) and bacteria (decreased), indicating differential responses between bacterial and fungal decomposers; (iv) evidence for phased nitrification and denitrification, driven by changes in soil dissolved oxygen; (v) evidence for organic sulfur processing (taurine) via bile salt hydrolases. This direct assessment of function expands the fundamental understanding of terrestrial vertebrate decomposition, providing insight into pathways of biogeochemical cycling within these hotspots.

Results

Soil Physiochemistry

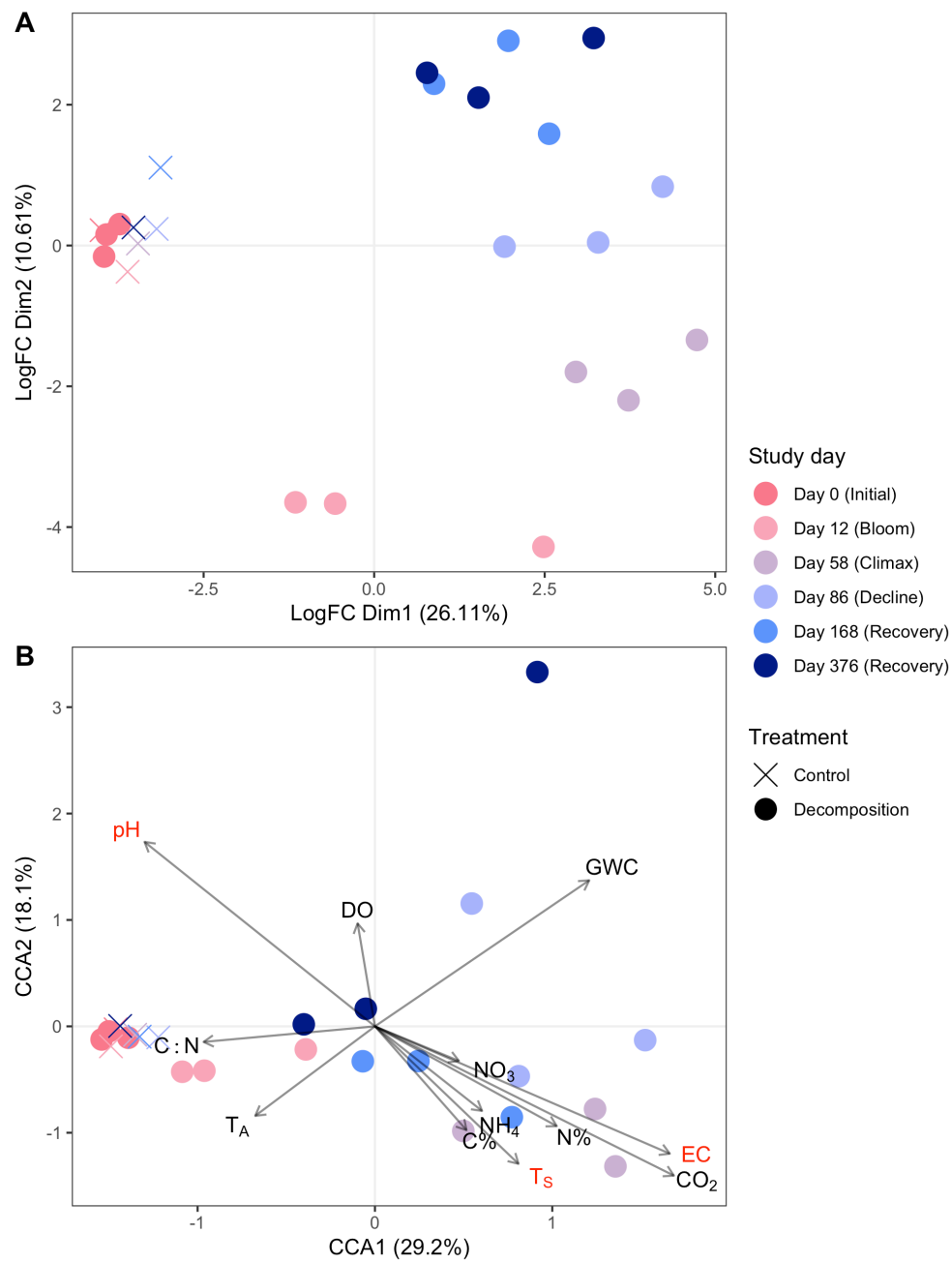
Soil chemistry was altered in response to the presence of decomposing human cadavers, with multiple parameters still impacted after one year [13]. Generally, soil pH decreased and remained low in decomposition soils. Soil electrical conductivity (EC) increased in response to decomposition, remaining elevated through approximately day 58 before gradually decreasing throughout the remainder of the study (Fig. S1). Respiration (evolved CO₂) increased by an order of magnitude beginning at day 12, which corresponded to a reduction in soil dissolved oxygen (DO) to 29% - 48.9%. Ammonium concentrations increased 78-fold, reaching maximum concentrations between days 12 and 58. This was followed by decreased ammonium and increased nitrate concentrations at day 86, with nitrate concentrations reaching a maximum at day 168 (Fig. S1).

Microbial gene expression in response to human decomposition

Gene expression profiles in decomposition-impacted soils shifted away from controls and day zero samples as decomposition progressed (Fig 1A). Expression was most different from controls on study days 58, 86, 168 (Fig. S2), before starting to return toward control conditions on study day 376. After one year of decomposition, soil gene

expression profiles had not returned to pre-decomposition conditions, as evidenced by their clustering away from controls and day zero samples in the MDS plot (Fig 1A).

Figure 1: Microbial gene expression profiles are altered during human decomposition. Multidimensional scaling (MDS) shows gene expression within soils changed as decomposition progressed (A). Canonical correspondence analysis (CCA) shows that environmental variables explained 47.3% of the variation in gene expression profiles (B). Variables in bold red type significantly ($p < 0.05$) explained some of the variation in gene expression profiles as assessed by Permutational Analysis of Variance (PERMANOVA). In both panels, treatment (control, decomposition) is denoted by shape, while color represents study day with associated decomposition phase (Fig. S5) in parentheses. In B, soil physiochemical variable loadings are represented by arrows: Gravimetric water content (GWC), electrical conductivity (EC), pH (pH), dissolved oxygen (DO), respiration (evolved CO_2 $\mu\text{mol gdw}^{-1}$), ammonium (NH_4), and nitrate (NO_3) concentrations (mg gdw^{-1}), percent carbon (%C), percent nitrogen (%N), carbon:nitrogen ratio (C:N), ambient temperature (T_A), and soil temperature (T_S).

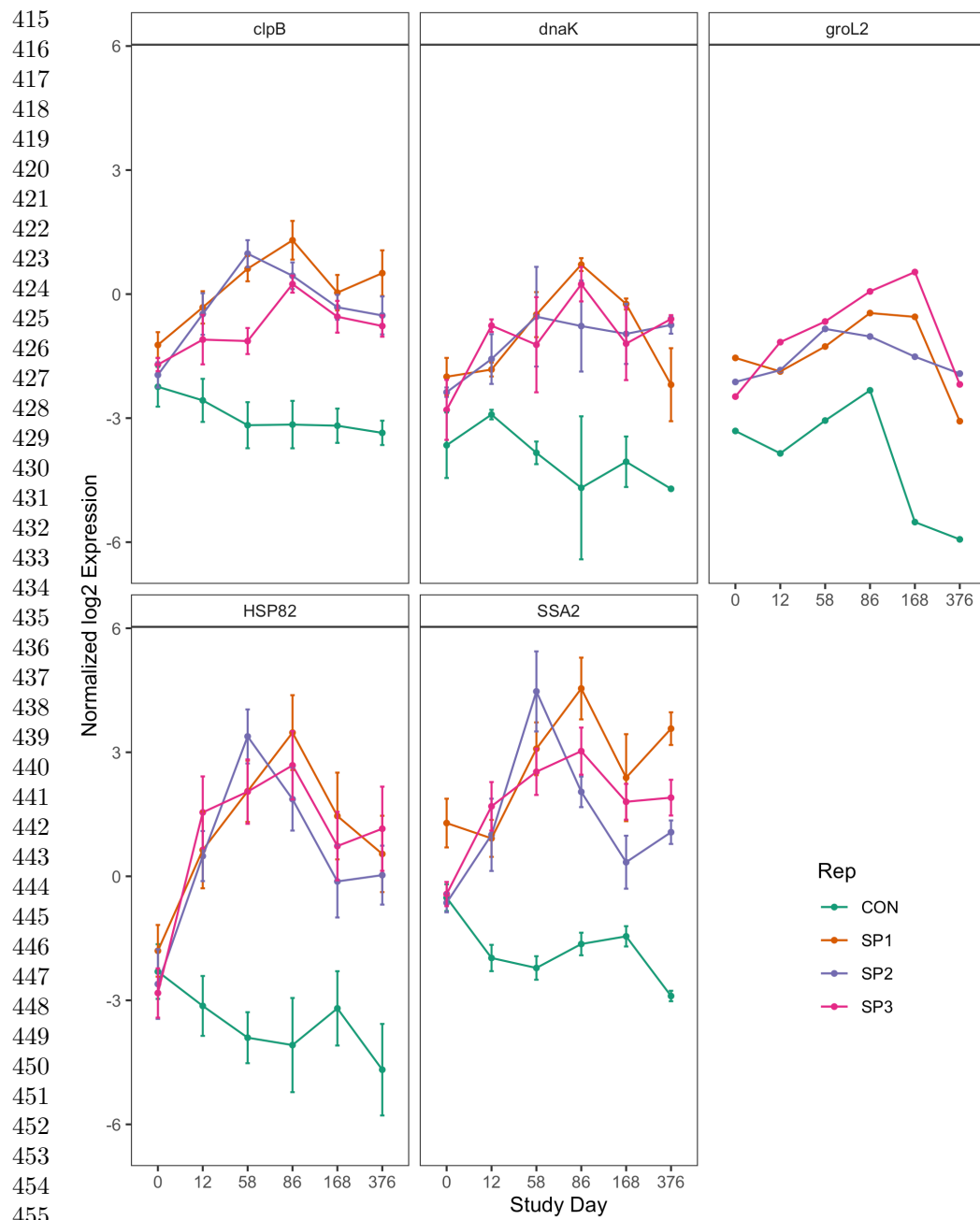


Some correlations were observed between gene expression shifts and soil physiochemical data at decomposition timepoints. Canonical correspondence analysis (CCA) was

323 used to constrain gene expression data with soil physiochemical data (Fig 1B). CCA1
 324 and CCA2 explained 29.2% and 18.1% of the variance in gene expression, respectively.
 325 Transcript profiles at day 12 were associated with an increase in soil carbon to nitrogen
 326 ratio (C:N). Gene expression profiles at days 58 to 86 were positively correlated with
 327 increased soil temperature, EC, and evolved CO₂, while study day 168 was associated
 328 with elevated levels of soil NO₃. Further, Permutational Analysis of Variance (PER-
 329 MANOVA) revealed that internal accumulated degree hours (ADH) ($p = 0.001$), soil
 330 temperature ($p = 0.039$), pH ($p = 0.033$), and EC ($p = 0.031$) significantly explained
 331 some of the variation in gene expression profiles ($p < 0.05$). No other soil chemical
 332 variables were significant at $\alpha = 0.05$ (Table S1).
 333
 334 Overall, decomposition changed soil gene expression profiles over the one-year study
 340 relative to control soils. Differential expression analysis between decomposition and
 341 control soils identified 7,047 down-regulated and 38,425 up-regulated genes. Gene
 342 transcripts that were associated with control soils belonged to a wide variety of clus-
 343 ters of orthologous genes (COG) functional categories. Specifically, the top 20 genes
 344 whose expression was higher in control soils belonged to ten unique COG categories,
 345 including signal transduction mechanisms, transcription, and those of unknown func-
 346 tion. In contrast, the top 20 genes whose expression was higher in decomposition
 347 soils only fell into four COG categories (Fig. S3 A): 1) post-translational modifica-
 348 tion, protein turnover, and chaperones; 2) energy production and conversion; 3) cell
 349 motility; and 4) carbohydrate transport and metabolism. The most common COG
 350 category represented in decomposition soils (80% of the top 20 genes) was post-
 351 translational modification, protein turnover, and chaperones. Within this category,
 352 several heat shock stress response genes were identified, including clpB, dnaK, groL2,
 353 SSA2, HSP82, and clpB (Table S2). Further investigation of these genes over time
 354 shows that their expression increased, typically reaching maximum transcript levels
 355 around study days 58 and 86 (Fig 2). This corresponded to elevated soil temperatures
 356
 357
 358
 359
 360
 361
 362
 363
 364
 365
 366
 367
 368

below decomposing bodies between study days 12-80, with soil temperatures increasing to approximately 43°C [13], as well as maximum soil EC and minimum dissolved oxygen measurements between days 12 and 58 (Fig. S1).

Figure 2: Mean normalized log2 expression of heat shock proteins identified by differential expression analysis comparing decomposition and control soils. Each panel represents a single heat shock gene, labeled with gene names, identified via Prodigal. Symbol color denotes if the sample is a control (CON, green), or one of three individuals: SP1 (orange), SP2 (purple), or SP3 (pink). Error bars are standard error of individual query genes in the top 20 transcripts associated with decomposition soils.



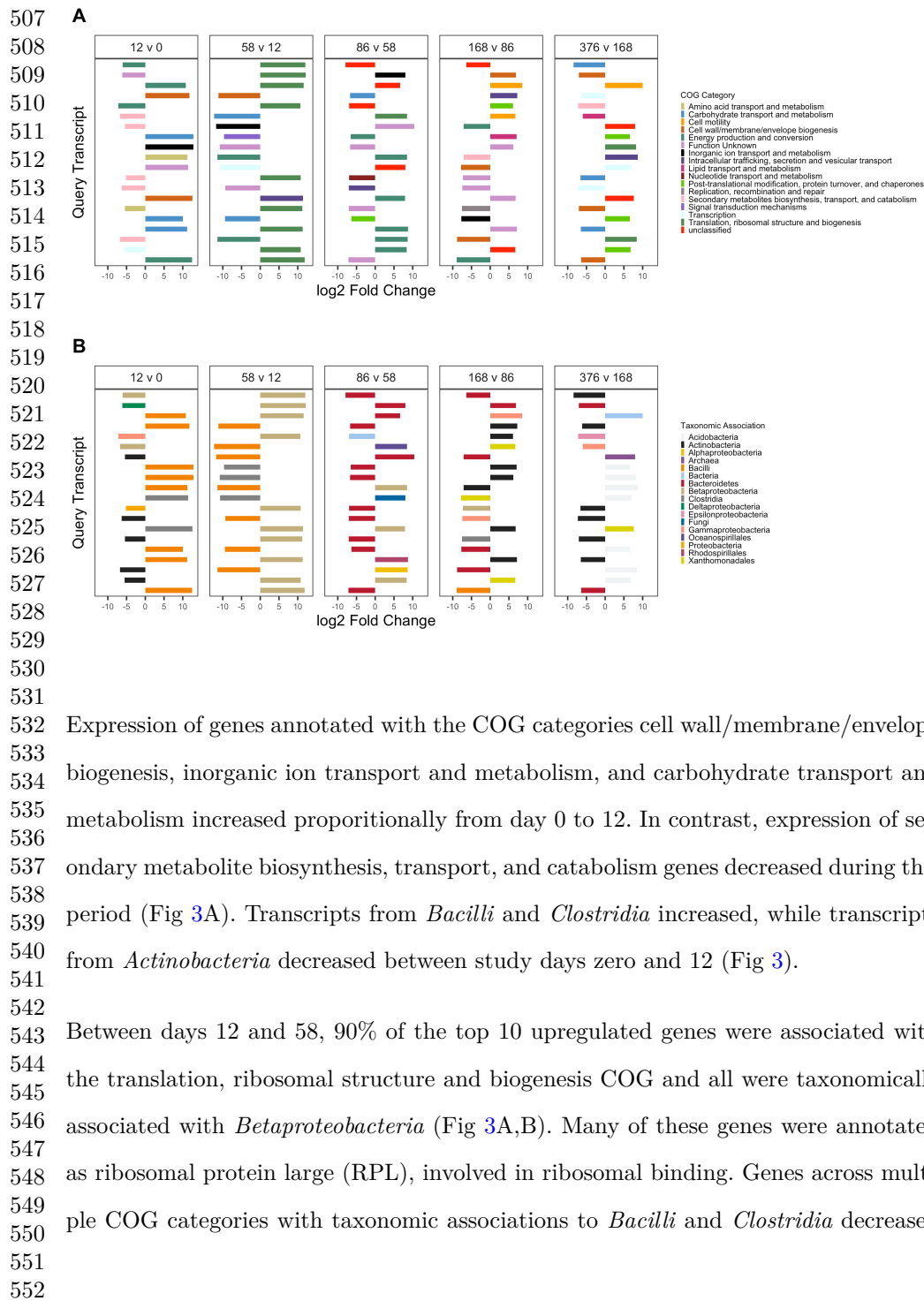
Taxonomy associated with top differentially expressed gene transcripts also differed between control and decomposition soils. The top 40 most significant differentially

expressed gene transcripts in decomposition soils were associated with Fungi, *Actinobacteria*, and *Xanthomonadales*, while gene transcripts in controls were associated with *Acidobacteria*, *Cyanobacteria*, *Proteobacteria* (α , δ , γ), and *Planctomycetes* (Fig. S3 B). The greatest number of differentially expressed genes relative to control samples was observed at day 86, where we saw 145,460 and 124,883 up- and down-regulated genes, respectively.

Temporal gene expression shows shifted decomposer functions

Differential expression analysis between sequential study days revealed which genes were altered during decomposition. The top ten transcripts that changed in representation (increased/decreased), determined by the lowest p-values from differential expression analysis, are reported in Table S3 and Fig 3.

Figure 3: Top twenty up- and down-regulated genes in decomposition soils comparing sequential study days (0, 12, 58, 86, 168, 376) colored by COG functional category (A) and taxonomic annotation (B). Positive values denote increased expression compared to the preceding timepoint, while negative values denote a decrease.



between study days 12 and 58, six of which were transcripts that previously increased between days zero and 12 (Fig 3B, Table S3).

Multiple transcripts associated with the energy production and conversion COG, as well as transcripts annotated as inorganic transport and metabolism, and translation, ribosomal structure and biogenesis, increased between days 58 and 86 (Fig 3A). Two of the upregulated energy and production and conservation transcripts were associated with cytochrome c oxidase subunits in *Betaproteobacteria*, while another was annotated as *hao*, encoding the enzyme hydroxylamine dehydrogenase which is involved in conversion of hydroxylamine to nitrite during nitrification (Table S3). Further investigation into hydroxylamine dehydrogenase showed a significant increase in *hao* transcripts at day 86 followed by subsequent decreases at days 168 and 376 ($F = 4.183$; $p = 0.02$). This increase corresponded to decreased soil ammonium levels and subsequent accumulation of nitrate (Fig. S1). Half of the 10 most downregulated genes between days 58 and 86 were not assigned to a COG (*i.e.*, unclassified) or were of unknown function.

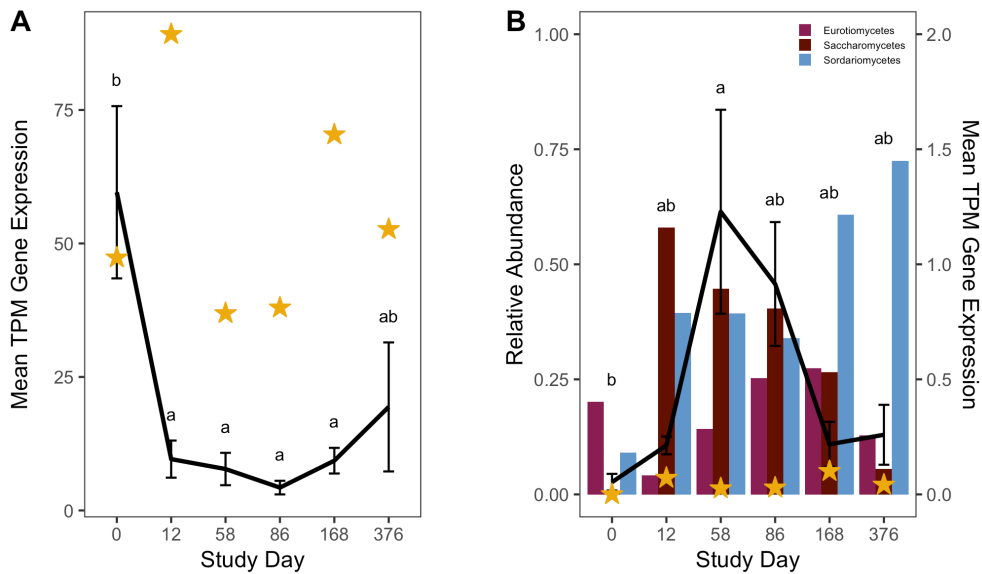
Differential expression comparing study days 86 with 168 and 168 with 376 identified genes across a variety of functional categories, with many unclassified in the COG database or with unknown function (Fig 3A). Expression of carbohydrate transport and metabolism genes associated with *Bacilli* decreased between day 168 and 376. *Acidobacteria* transcripts increased in decomposition-impacted soils between study day 168 and 376, but were not associated with any single COG category (Fig 3B).

Organic carbon metabolism

We expected to observe increased expression of lipid metabolizing genes during active and advanced decomposition as microbes degraded lipids deposited in the soil [19].

Therefore, we investigated changes in triacylglycerol lipase (enzyme commission number: 3.1.1.3) gene transcription in our soils. Generally, lipase transcripts decreased as decomposition progressed (HLM $F = 6.564$, $p < 0.001$), however we also observed a significant interaction between study day and taxonomic annotation ($F = 8.786$; $p < 0.001$). Specifically, lipase gene transcripts annotated as bacteria decreased with decomposition time ($F = 10.392$; $p = 0.001$), while fungal lipase transcripts increased, reaching a maximum at study day 58 ($F = 4.509$; $p = 0.015$) (Fig 4).

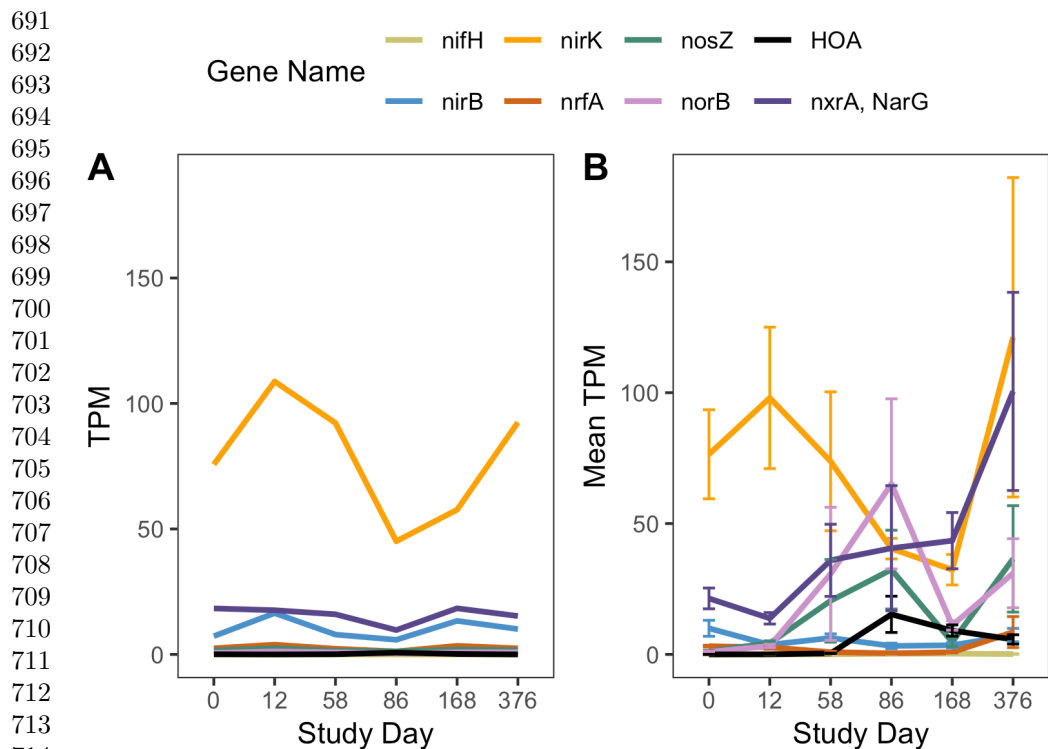
Figure 4: Mean transcript abundance, in transcripts per million (TPM), of all bacterial (A) and fungal (B) triacylglycerol lipase (EC 3.1.1.3) genes over time. Abundance of both bacterial ($p = 0.001$) and fungal ($p = 0.015$) lipase transcripts change significantly over time. Black lines (A, B) report mean and standard deviation of TPM from three individuals (black line), while gold stars denote mean TPM in control soils. Letters are the result of post-hoc Tukey tests between decomposition timepoints. In B, bars show the relative abundance of the fungal classes *Saccharomycetes*, *Sordariomycetes*, and *Eurotiomycetes*, reported in Taylor et al. (2024).



Nitrogen- and sulfur compound transformations

Expression of nitrogen cycling genes was impacted in response to human decomposition. Due to the detection of hydroxylamine oxidoreductase (*hao*) transcripts in our differential expression analysis, and our hypotheses predicting changes to nitrogen transformation processes, the expression of genes encoding common enzymes involved in nitrogen cycling (*nifH*, *nirB*, *nirK*, *norB*, *nosZ*, *nrfA*, *nxrA*, and *amoA*) were assessed using their enzyme commission numbers (Fig 5A,B). *nifH*, encoding a subunit of nitrogenase which is involved in nitrogen fixation, displayed little to no changes in gene expression between control and decomposition soils. Transcripts for two genes encoding enzymes contributing to the last two steps of denitrification, *norB* (nitric oxide reductase) and *nosZ* (nitrous oxide reductase), increased between study days 12 and 86, and decreased at study day 168 before increasing again at day 376. In contrast, expression of genes encoding nitrate reductase, *narG*, and NO-forming nitrite reductase, *nirK*, remained low until day 376 when transcripts for both genes increased. As noted above, expression of *hao*, encoding hydroxylamine dehydrogenase, increased at study day 86 before decreasing at remaining timepoints (Fig 3A, Fig 5B). Expression of *amoA*, encoding a subunit of ammonia monooxygenase, and *nxrA*, encoding a subunit of nitrite oxidoreductase, which are involved in nitrification, changed in response to decomposition. *amoA* transcripts initially decreased at day 12, remaining reduced until study day 376. Similarly, abundance of transcripts encoding enzymes involved in dissimilatory nitrate reduction, *nirB*, and *nrfA*, was low for the first 168 days, with *nrfA* expression increasing at day 376 (Fig 5B).

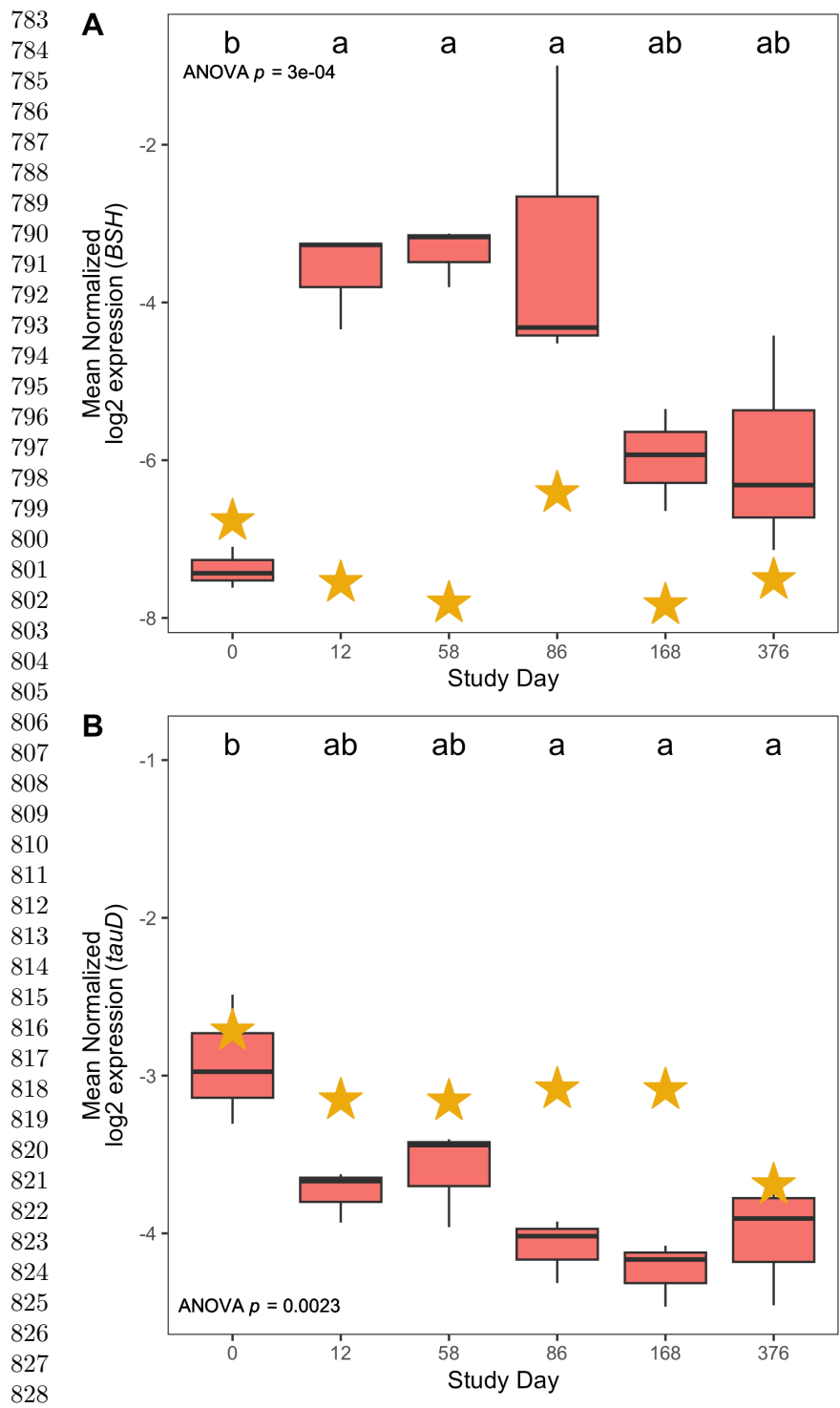
Figure 5: Mean gene expression, in transcripts per million (TPM), of commonly used marker genes for enzymes involved in nitrogen cycling over time in controls (A) and decomposition (B) soils. Data in B represent mean and standard deviation of TPM from three individuals.



Expression of genes involved in metabolism of nitrogen and sulfur-containing compounds were also impacted by human decomposition. Specifically, four of the top ten genes whose expression decreased at day 12 were related to taurine metabolism, with their annotations associated with *tauD*, encoding taurine dioxygenase. (Table S3). Further investigation into *tauD* showed that mean expression of these genes decreased steadily over one year, beginning at day 12 (Fig 6B); however, *tauD* expression in response to human decomposition was variable across taxonomic associations. Most *tauD* transcripts were associated with *Gammaproteobacteria*, *Actinobacteria*, *Betaproteobacteria*, *Alphaproteobacteria*, and fungi. While a majority of the *tauD* gene queries displayed reduced expression over time, expression of fungal-associated and a few *Betaproteobacteria*-associated *tauD* genes increased at day 58 (Fig. S4). Sources of taurine in the human body include taurine absorbed from the diet and taurine produced

from anaerobic microbial deconjugation of bile salts via bile salt hydrolase (BSH) enzymes [22]. Therefore, we examined transcripts encoding BSH enzymes in decomposition soils. Expression of these genes was elevated at days 12, 58, and 86 before converging toward pre-decomposition levels at days 168 and 376 (Fig 6A). Hierarchical linear mixed effects (HLM) models showed that both *tauD* (HLM $F = 7.356$, $p = 0.002$) and BSH ($F = 13.768$, $p < 0.001$) gene expression was significantly different over time (Fig 6A,B).

Figure 6: Mean bile salt hydrolase, BSH, (A) and *tauD*, taurine dioxygenase, (B) log2 normalized expression in controls (gold stars) and decomposition (boxplots) soils. Boxplots display the 25th and 75th quartiles and median log2 normalized values between all three individuals at each timepoint. ANOVA p-value is the result of a hierarchical linear mixed effects model accounting for repeated measures of each donor block, while letters denote the results of *post-hoc* Tukey test.



Discussion

The goal of this study was to assess microbial gene expression in soils responding to human decomposition. Metatranscriptomics were applied to soil samples collected over one year from below three decomposing human bodies. From this, we found that microbial gene expression reproducibly shifted over time. Additionally, we showed that gene expression profiles had not recovered to pre-decomposition conditions after one year. Comparison of control and decomposition expression profiles revealed that heat-shock proteins were elevated in response to decomposition. We also described expression patterns between decomposition timepoints, noting changes in functional gene categories at certain timepoints, in particular with respect to lipid, nitrogen and sulfur metabolism.

Decomposition impacted soil community gene expression for at least one year

Gene expression profiles remained altered after one year of decomposition. It is unclear if soil microbial communities, in terms of gene expression profiles, had reached a new steady state as a result of decomposition, or if they would eventually return to pre-decomposition conditions. The soil pH, EC, NH_4^+ , NO_3^- , and total nitrogen (TN) exhibited differences (although not statistically significant) in these soils following a year of decomposition, however bacterial and fungal community structures, as assessed by rRNA amplicon libraries, were still altered [13]. This indicates that decomposition can continue to structure microbial communities and impact their function for extended periods of time. While nutrient pools and communities both demonstrate less rapid change at later time points in the study, there is no evidence suggesting an arrival at a steady-state post-disturbance microbial community within our study. In some studies, human decomposition can result in elevated carbon and nutrients (organic nitrogen, ammonium, nitrate, and phosphate) for longer than a year [3], suggesting

875 decomposition events have long-lasting effects on the local ecosystem. Together, this
876 has implications for terrestrial ecosystem processing (*e.g.*, nutrient cycling, emission of
877 greenhouse gasses, etc.), as we show that decomposition alters functional metabolism
878 pathways within soil microbial communities. It is clear that extended sample collec-
879 tions beyond a single year are needed to address how long microbial communities
880 are affected, and whether there is a return to the original state or some new altered
881 community condition.
882

883 Bacteria, fungi, and archaea were all represented by expressed genes throughout
884 decomposition, suggesting that members of all three domains have the potential
885 to contribute to decomposition processes and nutrient cycling. While a majority of
886 annotated transcripts were identified as bacterial, fungal transcripts were the sec-
887 ond most abundant group. Fungal transcripts made up almost half (*e.g.*, seven of
888 the top fifteen) of the significantly differentially expressed genes associated with
889 decomposition-impacted soils. Additionally, with respect to expression shifts between
890 decomposition timepoints, fungal transcripts were among the topmost upregulated
891 genes at study day 86. This is not surprising as fungi are key decomposers, involved
892 in the degradation of organic matter in terrestrial ecosystems [23]. It was interesting
893 to see an increase in certain fungal transcripts, such as lipase, at study days 58 and 86
894 when soil oxygen began to recover. We would expect lipids to enter the soil as tissues
895 are broken down during decomposition, so we were surprised to see bacterial lipase
896 genes decrease during decomposition. This suggests that microbial activity in decom-
897 position soils may be constrained by the changing chemical environment, potentially
898 altered oxygen levels in the case of bacterial lipase gene expression. Prior work with
899 these same soils showed that soil oxygen concentration was a key driver of changes in
900 both bacterial and fungal community composition [13].
901
902
903
904
905
906
907
908
909
910
911
912
913
914
915
916
917
918
919
920

Increased stress response during decomposition	921
	922
Soil microbial communities expressed stress response genes in response to human	923
decomposition. Differential expression analysis identified increased expression of mul-	924
tipte heat shock proteins associated with the taxa <i>Xanthomonadales</i> , <i>Actinobacteria</i> ,	925
and fungi. Upon further investigation, expression of these genes increased through day	926
58 and remained high for the remainder of the year. Soil temperature was elevated rel-	927
ative to controls between study days 8 and 80, with maximum temperatures $>40^{\circ}\text{C}$,	928
while soil electrical conductivity increased up to $663\ \mu\text{S cm}^{-1}$ (16X higher than back-	929
ground) through day 58 before slowly decreasing through the remainder of the study.	930
Soil electrical conductivity correlates with ionic strength and can be an indicator	931
of increased salinity [24]. During vertebrate decomposition, elevated conductivity in	932
impacted soils is attributable to sodium (Na), potassium (K), and ammonium (NH_4)	933
[8–11, 13]. As a result, we would expect these microbes to be experiencing both heat	934
and osmotic stress during this period. Prior work has observed increased heat shock	935
gene expression during salt stress in paddy soils [25] and the presence of both heat	936
and osmotic stress genes in desert soils along a salt gradient [26], suggesting saline	937
conditions can alter the expression of heat and/or osmotic stress genes. In our study	938
we observed the stress response within soil microbial communities was stimulated dur-	939
ing human decomposition. At this time, however, it is unclear if expression of these	940
genes is in response to heat stress alone, or in combination with osmotic stress.	941
	942
	943
	944
Increased expression of fungal lipase genes during	945
decomposition	946
	947
Human fat tissue contains lipids that are broken down during decomposition. There-	948
fore, we assessed expression of triacylglycerol lipase genes in decomposition soils. Our	949
results show that expression of triacylglycerol lipase genes was altered in response	950
to decomposition, and these shifts differed between bacterial and fungal transcripts.	951
	952
	953
	954
	955
	956
	957
	958
	959
	960
	961
	962
	963
	964
	965
	966

Specifically, bacterial triacylglycerol lipase transcripts decreased in response to decomposition, while fungal triacylglycerol lipase transcripts increased. Further, expression of these genes corresponded to changes in relative abundance of the fungal classes *Saccharomycetes*, *Sordariomycetes*, and *Eurotiomycetes* [13]. These fungi have been previously associated with decomposition soils [27, 28] and are known to contain triacylglycerol lipase genes in their genomes [29, 30], suggesting that they play a role in lipid degradation in decomposition soils.

Our observation of an overall decrease in triacylglycerol lipase transcripts contrasts with previous work by Howard et al. (2010) [19], who observed increased copies of Group 1 lipase genes via qPCR during swine (*Sus scrofa*) decomposition. Fatty acid composition differs between human and pig tissue [31], potentially altering the lipid profile available for microbes, leading to differences in decomposition products within the soil [18]. These products can then directly or indirectly alter community composition and/or activity of functional proteins via substrate availability or the chemical environment. Further, in a side-by-side comparison of human and pig decomposition at the same location, soil pH increased under pigs, but decreased under humans [18]. Altered pH and soil chemistry could result in different functions and gene expression in decomposition-impacted soils. Many triacylglycerol lipases have a pH optimum that is neutral to basic [32–34], so cells may be decreasing expression under acidic conditions in human decomposition soils. Availability of lipid species and changes to pH may select for taxa that favor these substrates/pH conditions; for example, Mason et al. (2022) [12] showed a relationship between the abundance of the fungal taxa *Saccharomycetes* and antemortem body mass index (BMI) due to relative proportions of fat and muscle tissue.

Evidence for phased denitrification and nitrification	1013
	1014
The human body is a concentrated source of nitrogen that is released into the sur-	1015
rounding soil during decomposition. Expression of common marker genes for nitrogen	1016
cycling was altered in decomposition soil and suggested nitrogen transformations	1017
during human decomposition are driven by soil oxygen concentrations with hydroxy-	1018
lamine as an important intermediate. We observed low or reduced expression of the	1019
nitrification genes <i>nrrA</i> and <i>amoA</i> between days 12 and 86, during a period when	1020
oxygen was reduced to 39% - 85%. This was concomitant with an accumulation of	1021
ammonium, which reached a maximum on day 12, and low nitrate indicating that nitrifi-	1022
cation was inhibited. This period of reduced soil oxygen constraining nitrification	1023
was also described in a decomposition experiment with beaver (<i>Castor canadensis</i>)	1024
carcasses Keenan et al. (2018) [8].	1025
	1026
	1027
	1028
	1029
	1030
	1031
	1032
	1033
We observed increased gene expression for the enzyme hydroxylamine dehydrogenase	1034
(HAO) at day 86 while oxygen was reduced (~85%). This corresponded to simultane-	1035
ous increases in expression of genes encoding subunits of nitric oxide reductase (<i>norB</i>)	1036
and nitrous oxide reductase (<i>nosZ</i>). Traditionally HAO has been thought to process	1037
hydroxylamine to nitrite during nitrification, while nitric oxide reductase and nitrous	1038
oxide reductase are enzymes involved in the last two steps of denitrification converting	1039
nitric oxide (NO) to dinitrogen gas (N ₂). However, recent work suggested hydroxy-	1040
lamine can be converted to nitric oxide (NO), and can interact with multiple phases	1041
of the nitrogen cycle [35]. Even though <i>amoA</i> expression was shown to decrease dur-	1042
ing reduced oxygen conditions, <i>amoA</i> transcripts were still present and likely able	1043
to convert ammonium to hydroxylamine as soil oxygen was not completely depleted	1044
during decomposition. Additionally, a previous study reported that the growth of the	1045
ammonia oxidizing bacteria <i>Nitrosomonas europaea</i> under anoxic conditions lead to	1046
accumulation of hydroxylamine in a chemostat bioreactor [36], suggesting anaerobic	1047
	1048
	1049
	1050
	1051
	1052
	1053
	1054
	1055
	1056
	1057
	1058

1059 ammonium oxidation (anammox) may also be occurring in decomposition soils. How-
 1060 ever, we did not observe increases in *nirK* expression, which might suggest conversion
 1061 of nitrite to NO for use in the anammox pathway. NO produced via HAO activity may
 1062 be used for anammox in these soils; however, the role of hydroxylamine as an inter-
 1063 mediate in anammox is still debated [35]. Therefore, our current hypothesis is that
 1064 hydroxylamine accumulates under anaerobic conditions during decomposition, which
 1065 can then be converted to NO by HAO. This NO would then be present for anaerobic
 1066 denitrifying bacteria to convert to nitrous oxide (N₂O) by nitric oxide reductase and
 1067 finally to N₂ by nitrous oxide reductase. Keenan et al. (2018) [8] noted a brief increase
 1068 in N₂O emissions during beaver carcass decomposition, which suggests denitrification
 1069 was occurring during this phase of reduced soil oxygen concentrations.
 1070
 1071
 1072
 1073
 1074
 1075
 1076
 1077

1078 As soils fully reoxygenated by day 168, we observed increased expression of genes
 1079 encoding enzymes involved in aerobic nitrification, *amoA* and *nxrR*. Nitrification is
 1080 an oxygen-dependent process which would convert accumulated ammonium to nitrate;
 1081 the increase in nitrate concentrations may then serve as a substrate for denitrification.
 1082 We observed increased expression of marker genes encoding all four enzymes in the
 1083 complete dissimilatory denitrification pathway (*narG*, *nirK*, *norB*, and *nosZ*) at day
 1084 376. Increased expression of nitrification and denitrification marker genes is consistent
 1085 with the accumulation of nitrite, nitrate, and N₂O after oxygen is reintroduced to
 1086 soils described in Keenan et al. (2018) [3, 8]. Together, gene expression patterns in
 1087 our study provide further insight into nitrogen transformations in during vertebrate
 1088 decomposition, suggesting an important role of hydroxylamine.
 1089
 1090
 1091
 1092
 1093
 1094
 1095
 1096
 1097

1098 **Increased expression of bile salt hydrolases**

1099 Sulfur is present in various organic molecules, including taurine, a sulfur- and nitrogen-
 1100 rich compound involved in bile acid formation [22]. Taurine in the human body can
 1101 be absorbed from the diet or synthesized in the liver [37]. However, taurine is also
 1102
 1103
 1104

produced as a byproduct of the deconjugation of bile salts via bile salt hydrolases (BSHs) present in the anaerobic gut taxa *Lactobacillus* and *Clostridium* [22]. We observed increased expression of genes encoding BSH enzymes between days 12 and 86. Given that increased expression of BSH genes corresponded to the beginning of active decomposition, when decomposition products were observed to enter the soil, and the period of reduced dissolved oxygen in our study, it is likely that taurine accumulation is the result of BSH enzyme activity by anaerobic microorganisms. While we did not measure taurine concentrations in the present study, our results correspond to previous decomposition studies that report accumulation of taurine in various organs and body regions [38–40] and soils [18, 41] during decomposition via metabolomics, and increased relative abundance of *Clostridium* and *Lactobacillus* within the body [42–44] and in decomposition soils [20] via DNA sequencing methods, including in these soils [13].

Taurine can be metabolised through desulfurization via the α -ketoglutarate-dependent enzyme taurine dioxygenase (TauD). Specifically, this enzyme, encoded by the gene *tauD*, converts 2-oxoglutarate and taurine to produce aminoacetaldehyde, succinate, sulfite, and CO₂ [45]. Succinate and sulfite from this reaction can then be used for the citric acid cycle and sulfur metabolism, respectively. Given increased BSH expression in our study and reported taurine accumulation in others, we would expect taurine to be present for microbial metabolism by TauD. However, we observed a general decrease in *tauD* expression between days 12 through 376. This trend was driven by reduced expression of *tauD* transcripts associated with *Proteobacteria*, *Gammaproteobacteria*, and *Actinobacteria* whose relative abundance have been shown to remain consistent or increase during human decomposition [20], suggesting that *tauD* expression is downregulated under decomposition conditions. However, we noted that expression of *tauD* genes associated with fungi and a few *Betaproteobacteria* displayed increased representation at day 58, corresponding to increased expression of

1151 bile salt hydrolases (BSH) between days 12 and 86. The reduction in *tauD* expres-
1152 sion may be due to increased sulfur availability. We did not measure sulfur species
1153 in this experiment; however, others have observed increased sulfur concentrations in
1154 decomposition-impacted soils [3, 7, 11]. Thus, sulfur scavenging pathways such as tau-
1155 rine desulfurization by TauD [46], whose genes are expressed under sulfur-limiting
1156 conditions, likely display reduced expression under sulfur replete conditions. Addition-
1157 ally, taurine may be processed through other pathways. For example, taurine can be
1158 deaminated by taurine dehydrogenase to produce sulfite and acetyl-CoA for carbon
1159 metabolism [45, 47]. Overall, our results suggest that human decomposition has poten-
1160 tial impacts on soil sulfur biogeochemistry through deposition of inorganic (sulfate)
1161 and organic (sulfur-containing amino acids) sulfur compounds.

1169 1170 1171 **Conclusion**

1172
1173 This study investigated soil microbial gene expression during human decomposition.
1174 Metatranscriptomic analysis of soils from three human individuals shows that decom-
1175 position impacted microbial community gene expression profiles, exhibiting functional
1176 shifts over one year. This included altered expression of genes involved in lipid, N
1177 and S metabolism as microbes processed the nutrient-rich tissues of the human body.
1178 Additionally, we noted that functionality within decomposition-impacted soils was
1179 still affected after one year and had not returned to starting or background condi-
1180 tions. Together, these results show that vertebrate decomposition has lasting impacts
1181 on local soil ecosystems, including soil microbial communities. These results have
1182 important implications for understanding biogeochemical changes due to vertebrate
1183 mortality events in terrestrial ecosystems.

1191
1192
1193
1194
1195
1196

Materials and Methods

Study design

In February 2018, three deceased male human subjects (hereafter, “donors”) were placed supine on the soil surface at the University of Tennessee Anthropology Research Facility (ARF) and allowed to decompose. Located in Knoxville, TN (35° 56’ 28” N, 83° 56’ 25” W) the ARF is a roughly 2-acre outdoor facility dedicated to studying human decomposition [48]. The soils at the ARF are comprised of the Loyston-Talbott-Rock outcrop (LtD) and Coghill-Corryton (CcD) complexes. LtD soils are a silty clay loam and channery clay overlaying lithic bedrock, while CcD soils are comprised of clay from weathered quartz limestone [13, 48]. A site that had not been previously exposed to decomposition was used for this study.

The decomposition field experiment is fully described in Taylor et al. (2024) [13]. Briefly, experiments were conducted in a block design, where each block consisted of one decomposition site and one control site [13]. In total three blocks, *i.e.*, three donors paired with three respective control sites, were included in the study. Each control site was chosen in a manner to ensure their location was uphill and roughly 2 m away from decomposition sites [13]. Donor internal temperatures were recorded by probes located in the abdomen, while ambient air temperatures were monitored via sensors located roughly 50 cm above the soil surface. Soil temperature and salinity were measured with sensors placed directly underneath each individual (Decagon Devices, GS3) [13]. Donors ranged from 65 to 86 in age and were within 1 kg of each other with regard to weight (90.7 to 91.6 kg); donor BMI varied between 27.7 to 29.6 [13].

1243 **Sampling and physiochemistry**

1244

1245 Decomposition of all subjects was observed for one year. During the one-year study
1246 period, soils were sampled at 20 timepoints chosen to correspond with morpho-
1247 logical stages of decomposition as described by Payne (1965) [49]. Once advanced
1248 decay was reached, soils were collected at intervals of 350 accumulated degree days
1249 (ADD), calculated using ambient air temperatures, up to one year. All soil cores
1250 were taken using a 1.9 cm (3/4 inch) diameter soil auger to a depth of 16 cm. Soils
1251 were divided into two depth fractions: 0-1 cm (interface) and 1-16 cm (core) for the
1252 analyses reported in Taylor et al. (2024) [13]; the entire 0 to 16 cm core was used
1253 for this current study. Decomposition soils were taken from directly beneath the
1254 cadavers, taking care to not re-sample the same location more than once. At the
1255 time of sampling, soil dissolved oxygen was measured in triplicate using an Orion
1256 Star™ A329 pH/ISE/Conductivity/Dissolved Oxygen portable multiparameter meter
1257 (ThermoFisher) [13].

1266

1267 A subset of 6 study timepoints were chosen for metatranscriptomics analysis. Study
1268 days 0, 12, 58, 86, 168, and 376 were chosen as they represented distinct biogeochem-
1269 ical phases during decomposition (Fig. S5). Study day 0 was chosen as a baseline
1270 sample prior to cadaver placement. Study day 12 was the start of active decompo-
1271 sition, during the initial bloom when soil microbial activity was rapidly increasing
1272 resulting in the onset of hypoxia: soil ammonium reached maximum concentrations
1273 and soil oxygen was at minimum (approximately 39%). Study day 58 was during a
1274 climax period of sustained elevated microbial activity, characterized by high ammo-
1275 nium concentrations, hypoxia, maximum soil temperatures and minimum soil pH [13].
1276 Study day 86 represented a period of declining microbial activity, declining hypoxia,
1277 and increasing nitrate concentrations. Study day 168 was chosen as nitrate was at its
1278 maximum and soil dissolved oxygen had recovered to 99%. Finally, day 376 was cho-
1279 sen to represent the end of the study, 1 year since cadaver placement. Each study day

1288

was represented by four soil samples for RNA extraction: one pooled control sample
which was a mix of the three control locations, plus one sample from each of the three
donors, yielding a total of 24 samples for this study.

Soil samples were transported to the University of Tennessee (Knoxville, TN) and
processed within 24 hours of collection. Soils were homogenized by hand to remove
insect larvae, roots, rocks, and other debris (> 2 mm). A subset of soils were used
to measure pH, electrical conductivity (EC), and evolved CO_2 as described in Tay-
lor (2024). Soil nitrogen species (NH_4^+ , NO_3^-) and total carbon (TC) and nitrogen
(TN) were measured in all soil samples as described in [13]. Reported values for soil
physiochemistry represent the full 16 cm core; estimated by summing interface and
core values reported by Taylor et. al, (2024) [13] in 1:16 and 15:16 ratios, respectively.
Control values reported here are means of the three experimental controls that were
unimpacted by decomposition.

Roughly 10 g of soil was reserved for nucleic acid extraction, placed in a 4 oz. Whirl-
Pak™ bag (Nasco), flash frozen in liquid nitrogen, and stored at -80°C until further
analysis. Bacterial and fungal community composition was assessed via amplicon
sequencing of the 16S rRNA gene and ITS2 region as described in Taylor et al. (2024).

RNA Extraction and Sequencing

RNA was extracted from 2 g of soil using Qiagen's RNeasy® PowerSoil® Total RNA
kit. Manufacturer's instructions were followed with a few modifications. Soils became
saline during decomposition; therefore, we followed the manufacturer's suggestion and
incubated all extracts at -20°C following addition of solution SR4 (step 9) to decrease
salt precipitation. All RNA samples were resuspended in 40 μl of Solution SR7. RNA
concentrations were assessed fluorometrically using the Qubit® RNA HS assay (cat-
alog no. Q32852) with 1 μl of RNA. DNA contamination was removed by DNase

1335 treating RNA extracts twice using Qiagen’s DNase Max® kit in 50 µl reactions. RNA
1336 concentrations were remeasured after DNase treatment. PCR with V4 16S rRNA gene
1337 primers [50, 51] was conducted using RNA extracts as the template to confirm removal
1338 of all DNA prior to sequencing. RNA aliquots were shipped to HudsonAlpha Dis-
1341 covery (Huntsville, AL) for library preparation and RNA sequencing. Dual-indexed
1342 libraries were prepared using the Illumina® Stranded Total RNA prep with riboso-
1343 mal RNA depletion via ligation with Ribo-Zero Plus. Libraries were then pooled and
1346 sequenced on Illumina’s NovaSeq 6000 v4 platform, resulting in demultiplexed fastq
1348 files for each sample.

1351 Bioinformatics

1352
1353 Illumina sequencing of the 24 libraries yielded a total of 5,073,476,730 reads, or
1354 2,536,738,365 paired reads, with a mean of 105,697,432 paired reads per sample. Read
1355 quality control (QC) was conducted in KBase [52] using Trimmomatic [53]. Paired
1356 fastq files were imported to KBase through Globus. Poor quality reads were removed
1357 (4.7% of all reads), and adapters trimmed via Trimmomatic (v0.36) using default set-
1360 tings and the TruSeq3-PE-2 adapter file, resulting in 4,834,123,062 total reads. After
1361 QC check with FastQC, trimmed libraries were exported as fastq files from KBase
1362 through Globus. Remaining ribosomal RNA was filtered using bbmap (maxindel =
1363 20, minid = 0.93) from the Joint Genome Institute’s (JGI) bbtools suite [54]. Fil-
1364 tering of ribosomal RNA further removed 7.3% of reads, leaving 4,479,804,360 reads
1365 for assembly. Following this step, all non-ribosomal reads from all 24 samples were
1366 merged into one file. Reads were then co-assembled into contigs using the de novo
1367 assembler MEGAHIT (v1.2.9) [55] (−12 −k-min 23, −k-max 123, −k-step 10).

1375
1376 Gene identification and annotation from co-assembled contigs was performed using
1377 Prodigal [56] and eggNOG mapper [57], respectively. Briefly, the DNA fasta contain-
1378 ing all contigs was submitted to Prodigal (v2.6.3) for protein coding gene predication
1379

for a meta-sample (-p meta -f gff). After co-assembly, a total of 6,257,674 gene calls were identified by Prodigal. Next, predicated genes were functionally and taxonomically annotated using eggNOG mapper (v2.1.6) using basic settings to perform a diamond blastp search [58]. From this, 1,048,573 proteins were annotated by eggNOG-mapper (16.7%). Most of the annotated proteins were taxonomically annotated as bacteria (91.3%), followed by eukaryotes (7.6 %), and archaea (0.81 %). Of the 7.6% of eukaryotic proteins, 64.4% (4.9% of all proteins) were annotated as fungi. For this study, genes of interest included all bacterial, archaeal, and fungal proteins, therefore all non-fungal eukaryotic proteins (32,004) were removed prior to downstream analysis. Transcript counts for all genes of interest were obtained by mapping reads from each respective sample to genes of interest obtained from co-assembly using QIAGEN CLC Genomics Workbench 20.0 (<https://digitalinsights.qiagen.com/>). The percent of reads mapped to genes of interest ranged from 21% to 38% between samples, with an average of 31% reads mapped. Gene counts were then combined in a single file and used for downstream analyses in R.

Differential Expression

Transcript counts from all samples were combined in a single workable data file and imported into R for differential expression analysis using the R packages edgeR [59] and limma [60] following a modified pipeline by Phipson et al. (2020) [61]. The transcript count table was imported into R and converted to a DGElist object. Genes without sufficient counts for statistical analysis were removed to increase power using the edgeR function filterByExpr(), using study day as the comparison group.

Raw counts were then log2 normalized and gene expression profiles compared via multidimensional scaling (MDS) and hierarchical clustering. Multidimensional scaling (MDS) was conducted using plotMDS() from the limma package to assess differences between samples. MDS values were extracted from the MDS object, and the first two

1427 dimensions plotted using ggplot2 [62]. We also assessed the relationship between gene
 1428
 1429 expression profiles and changes in the soil environment using canonical correspondence
 1430 analysis (CCA). Environmental variables of interest included decomposition time in
 1431
 1432 accumulated degree hours (ADH) based on ambient temperatures, ADH based on
 1433
 1434 internal gut temperatures, ADH based on soil temperatures, gravimetric moisture,
 1435 pH, electrical conductivity (EC), dissolved oxygen (DO), CO₂ (μmol gdw⁻¹), NH₄ (mg
 1436
 1437 gdw⁻¹), NO₃ (mg gdw⁻¹), N %, C %, and CN ratio. First, permutational multivariate
 1438
 1439 analysis of variance (PERMANOVA) with adonis() (vegan v2.6.7) [63] was used to
 1440
 1441 identify significant soil parameters. Then the vegan functions cca() and scores() were
 1442
 1443 applied to run the CCA and extract scores, respectively. Scores for the first two
 1444
 1445 dimension were plotted using ggplot2, with loadings extracted from the CCA biplot.
 1446
 1447 For differential expression analysis, raw filtered reads were normalized using edgeR's
 1448
 1449 trimmed mean of M values (TMM) normalization using the function calcNormFac-
 1450
 1451 tors(). TMM normalized reads were then log2 transformed using limma's voom() and
 1452
 1453 differential expression assessed. Empirical Bayes shrinkage was used correct to p-
 1454
 1455 values for false discovery rates. The topmost up and down regulated genes for each
 1456
 1457 comparison, determined by log2 fold change and adjusted p-values, were then reported.
 1458
 1459 Expression of certain genes were assessed after performing transcripts per million
 1460
 1461 (TPM) normalization and statistical analyses with a combination of analysis of vari-
 1462
 1463 ance (ANOVA) and post-hoc Tukey tests. ANOVA across all timepoints were applied
 1464
 1465 to hierarchical linear mixed effects models to account for repeated sampling within
 1466
 1467 each donor block.

1466 Ethics approval and consent to participate

1468 All individuals were whole body donors to the Forensic Anthropology Center
 1469
 1470 (<https://fac.utk.edu/body-donation/>) specifically for the purpose of decomposition
 1471
 1472 research. No living human subjects were involved and only donors who consent to

decomposition research on their donation paperwork were enrolled in this study. The
University of Tennessee, Knoxville, Human Research Protections Program (HRPP)
reviewed this project and determined that research with human donors is exempt
under 45 CFR 46.101.

Consent for publication

No living human subjects were involved and only donors who consent to decomposition
research on their donation paperwork were enrolled in this study.

Funding

This research was funded by a National Institute of Justice Award (DOJ-NIJ-2017-
R2-CX-0008) to LST and JMD.

Availability of data and materials

Raw RNA sequence files from the Illumina Novaseq are available at the National Cen-
ter for Biotechnology Information's (NCBI) Sequence Read Archive (SRA) as a part
of [BioProject PRJNA1066312](#) under BioSample accession numbers SAMN45195141-
SAMN45195164. Additional datasets supporting the conclusions of this article are
available on [GitHub](#). Scripts containing code for all analyses and to generate figures
are available on [GitHub](#).

Competing interests

The authors declare that they have no competing interests.

1519 Authors' contributions

1520

1521 Conceptualization: ARM, LST, JMD; Methodology: ARM, LST, NEG, SWW, JMD;
1522

1523 Investigation: ARM, LST, JMD; Formal Analysis: ARM; Resources: JMD, SWW;

1524

1525 Data Curation: ARM; Writing – Original Draft: ARM, JMD; Writing – Review &

1526

1527 Editing: LST, NEG, SWW, JMD; Visualization: ARM; Supervision: JMD; Project

1528

1529 Administration: JMD; Funding Acquisition: LST, JMD. All authors read and approved

1530

1531 the final manuscript.”

1532

1533

1533 Acknowledgements

1534

1535 We would like to thank the Forensic Anthropology Center at the University of
1536

1537 Tennessee-Knoxville for their help in setting up field experiments. We would like to

1538

1539 thank Mary Davis for her help in managing the field site and helping to obtain donors

1540

1541 for this work.

1542

1543

1543 References

1544

1545

1546 [1] Benninger, L. A., Carter, D. O. & Forbes, S. L. The biochemical alteration of soil
1547 beneath a decomposing carcass. *Forensic Science International* **180**, 70–5 (2008).

1548

1549 [2] Towne, E. G. Prairie vegetation and soil nutrient responses to ungulate carcasses.
1550 *Oecologia* **122**, 232–239 (2000).

1551

1552

1553 [3] DeBruyn, J. M., Keenan, S. W. & Taylor, L. S. From carrion to soil: microbial
1554 recycling of animal carcasses. *Trends in Microbiology* **33**, 194–207 (2025).

1555

1556

1557 [4] Parmenter, R. R. & MacMahon, J. A. Carrion decomposition and nutrient cycling
1558 in a semiarid shrub–steppe ecosystem. *Ecological Monographs* **79**, 637–661 (2009).

1559

1560

1561

1562

1563

1564

[5] Macdonald, B. C. T. <i>et al.</i> Carrion decomposition causes large and lasting effects on soil amino acid and peptide flux. <i>Soil Biology and Biochemistry</i> 69 , 132–140 (2014).	1565 1566 1567 1568 1569 1570
[6] Bump, J. K. <i>et al.</i> Ungulate carcasses perforate ecological filters and create biogeochemical hotspots in forest herbaceous layers allowing trees a competitive advantage. <i>Ecosystems</i> 12 , 996–1007 (2009).	1571 1572 1573 1574 1575 1576
[7] Aitkenhead-Peterson, J. A., Owings, C. G., Alexander, M. B., Larison, N. & Bytheway, J. A. Mapping the lateral extent of human cadaver decomposition with soil chemistry. <i>Forensic Science International</i> 216 , 127–34 (2012).	1577 1578 1579 1580 1581 1582
[8] Keenan, S. W., Schaeffer, S. M., Jin, V. L. & DeBruyn, J. M. Mortality hotspots: nitrogen cycling in forest soils during vertebrate decomposition. <i>Soil Biology and Biochemistry</i> 121 , 165–176 (2018).	1583 1584 1585 1586 1587 1588
[9] Fancher, J. P. <i>et al.</i> An evaluation of soil chemistry in human cadaver decomposition islands: Potential for estimating postmortem interval (PMI). <i>Forensic Science International</i> 279 , 130–139 (2017).	1589 1590 1591 1592 1593 1594
[10] Quaggiotto, M.-M., Evans, M. J., Higgins, A., Strong, C. & Barton, P. S. Dynamic soil nutrient and moisture changes under decomposing vertebrate carcasses. <i>Biogeochemistry</i> 146 , 71–82 (2019).	1595 1596 1597 1598 1599 1600
[11] Taylor, L. S. <i>et al.</i> Soil elemental changes during human decomposition. <i>PLoS ONE</i> 18 , 1–24 (2023). Publisher: Public Library of Science.	1601 1602 1603 1604
[12] Mason, A. R. <i>et al.</i> Body mass index (BMI) impacts soil chemical and microbial response to human decomposition. <i>mSphere</i> e0032522 (2022).	1605 1606 1607 1608 1609 1610

1611 [13] Taylor, L. S. *et al.* Transient hypoxia drives soil microbial community dynamics
1612 and biogeochemistry during human decomposition. *FEMS Microbiology Ecology*
1613 **100**, fae119 (2024).
1614
1615
1616
1617 [14] Keenan, S. W., Emmons, A. L. & DeBruyn, J. M. Microbial community coa-
1618 lesence and nitrogen cycling in simulated mortality decomposition hotspots.
1619 *Ecological Processes* **12**, 45 (2023).
1620
1621
1622
1623 [15] Mason, A. R., Taylor, L. S. & DeBruyn, J. M. Microbial ecology of vertebrate
1624 decomposition in terrestrial ecosystems. *FEMS Microbiology Ecology* **99**, fiad006
1625 (2023).
1626
1627
1628 [16] Burcham, Z. M. *et al.* Total RNA analysis of bacterial community structural
1629 and functional shifts throughout vertebrate decomposition. *Journal of Forensic*
1630 *Sciences* **64**, 1707–1719 (2019).
1631
1632
1633
1634 [17] Ashe, E. C., Comeau, A. M., Zejdlik, K. & O’Connell, S. P. Characterization of
1635 bacterial community dynamics of the human mouth throughout decomposition
1636 via metagenomic, metatranscriptomic, and culturing techniques. *Frontiers in*
1637 *Microbiology* **12**, 689493 (2021).
1638
1639
1640
1641
1642 [18] DeBruyn, J. M. *et al.* Comparative decomposition of humans and pigs: soil biogeo-
1643 chemistry, microbial activity and metabolomic profiles. *Frontiers in Microbiology*
1644 **11**, 608856 (2021).
1645
1646
1647
1648 [19] Howard, G. T., Duos, B. & Watson-Horzelski, E. J. Characterization of the
1649 soil microbial community associated with the decomposition of a swine carcass.
1650 *International Biodeterioration & Biodegradation* **64**, 300–304 (2010).
1651
1652
1653 [20] Cobaugh, K. L., Schaeffer, S. M. & DeBruyn, J. M. Functional and structural
1654 succession of soil microbial communities below decomposing human cadavers.
1655
1656

Plos One **10**, e0130201 (2015). 1657
1658

[21] Singh, B. *et al.* Temporal and spatial impact of human cadaver decomposition 1659
on soil bacterial and arthropod community structure and function. *Frontiers in* 1660
Microbiology **8**, 2616 (2018). 1661
1662
1663
1664

[22] Urdaneta, V. & Casadesús, J. Interactions between bacteria and bile salts in the 1665
gastrointestinal and hepatobiliary tracts. *Frontiers in Medicine* **4** (2017). 1666
1667
1668

[23] van der Wal, A., Geydan, T. D., Kuyper, T. W. & de Boer, W. A thready affair: 1669
linking fungal diversity and community dynamics to terrestrial decomposition 1670
processes. *FEMS Microbiology Reviews* **37**, 477–494 (2013). 1671
1672
1673
1674

[24] Essington, M. E. *Soil and water chemistry: an integrative approach* (CRC press, 1675
2015). 1676
1677
1678

[25] Peng, J., Wegner, C.-E. & Liesack, W. Short-term exposure of paddy soil micro- 1679
bial communities to salt stress triggers different transcriptional responses of key 1680
taxonomic groups. *Frontiers in Microbiology* **8** (2017). 1681
1682
1683
1684

[26] Pandit, A. S. *et al.* A snapshot of microbial communities from the Kutch: one of 1685
the largest salt deserts in the World. *Extremophiles* **19**, 973–987 (2015). 1686
1687
1688

[27] Metcalf, J. L. *et al.* Microbial community assembly and metabolic function during 1689
mammalian corpse decomposition. *Science* **351**, 158–62 (2016). 1690
1691
1692

[28] Fu, X. *et al.* Fungal succession during mammalian cadaver decomposition and 1693
potential forensic implications. *Scientific Reports* **9**, 12907 (2019). 1694
1695
1696
1697

[29] Dujon, B. *et al.* Genome evolution in yeasts. *Nature* **430**, 35–44 (2004). 1698
1699
1700
1701
1702

1703 [30] Haridas, S. *et al.* The genome and transcriptome of the pine saprophyte *Ophios-*
1704 *toma piceae*, and a comparison with the bark beetle-associated pine pathogen
1705 *textitGrosmannia clavigera*. *BMC Genomics* **14**, 373 (2013).
1706
1707
1708
1709 [31] Notter, S. J., Stuart, B. H., Rowe, R. & Langlois, N. The initial changes of fat
1710 deposits during the decomposition of human and pig remains. *Journal of Forensic*
1711 *Sciences* **54**, 195–201 (2009).
1712
1713
1714 [32] Kok, R. G. *et al.* Characterization of the extracellular lipase, LipA, of *Acineto-*
1715 *bacter calcoaceticus* BD413 and sequence analysis of the cloned structural gene.
1716 *Molecular Microbiology* **15**, 803–818 (1995).
1717
1718
1719
1720 [33] Hasan, F., Shah, A. A. & Hameed, A. Influence of culture conditions on lipase
1721 production by *Bacillus* sp. FH5. *Annals of Microbiology* **56**, 247–252 (2006).
1722
1723
1724 [34] Zouaoui, B. & Bouziane, A. Production, optimization and characterization of
1725 the lipase from *Pseudomonas aeruginosa*. *Romanian Biotechnological Letters* **17**,
1726 7187–7193 (2012).
1727
1728
1729
1730 [35] Soler-Jofra, A., Pérez, J. & van Loosdrecht, M. C. M. Hydroxylamine and the
1731 nitrogen cycle: A review. *Water Research* **190**, 116723 (2021).
1732
1733
1734 [36] Yu, R., Perez-Garcia, O., Lu, H. & Chandran, K. *Nitrosomonas europaea* adapta-
1735 tion to anoxic-oxic cycling: Insights from transcription analysis, proteomics and
1736 metabolic network modeling. *Science of the Total Environment* **615**, 1566–1573
1737 (2018).
1738
1739
1740
1741
1742 [37] Seidel, U., Huebbe, P. & Rimbach, G. Taurine: A regulator of cellular redox
1743 homeostasis and skeletal muscle function. *Molecular Nutrition & Food Research*
1744 **63**, 1800569 (2019).
1745
1746
1747
1748

- [38] Mora-Ortiz, M., Trichard, M., Oregioni, A. & Claus, S. P. Thanatometabolomics: introducing NMR-based metabolomics to identify metabolic biomarkers of the time of death. *Metabolomics* **15**, 37 (2019).
- [39] Locci, E. *et al.* A ¹H NMR metabolomic approach for the estimation of the time since death using aqueous humour: an animal model. *Metabolomics* **15**, 76 (2019).
- [40] Zelentsova, E. A. *et al.* Post-mortem changes in the metabolomic compositions of rabbit blood, aqueous and vitreous humors. *Metabolomics* **12**, 172 (2016).
- [41] Hoeland, K. M. *Investigating the potential of postmortem metabolomics in mammalian decomposition studies in outdoor settings*. Ph.D. thesis, University of Tennessee-Knoxville, https://trace.tennessee.edu/utk_graddiss/7000 (2021).
- [42] Javan, G. T. *et al.* Human thanatobiome succession and time since death. *Scientific Reports* **6**, 29598 (2016).
- [43] Javan, G. T., Finley, S. J., Smith, T., Miller, J. & Wilkinson, J. E. Cadaver thanatobiome signatures: the ubiquitous nature of *Clostridium* species in human decomposition. *Frontiers in Microbiology* **8**, 2096 (2017).
- [44] DeBruyn, J. M. & Hauther, K. A. Postmortem succession of gut microbial communities in deceased human subjects. *PeerJ* **5**, e3437 (2017).
- [45] Cook, A. M. & Denger, K. *Metabolism of taurine in microorganisms*, 3–13 (2006).
- [46] Kertesz, M. A. Riding the sulfur cycle – metabolism of sulfonates and sulfate esters in Gram-negative bacteria. *FEMS Microbiology Reviews* **24**, 135–175 (2000).
- [47] Brüggemann, C., Denger, K., Cook, A. M. & Ruff, J. Enzymes and genes of taurine and isethionate dissimilation in *Paracoccus denitrificans*. *Microbiology*

1795 **150**, 805–816 (2004).
1796
1797 [48] Keenan, S. W. *et al.* Spatial impacts of a multi-individual grave on microbial
1798 and microfaunal communities and soil biogeochemistry. *PLoS One* **13**, e0208845
1799 (2018).
1800
1801
1802
1803 [49] Payne, J. A. A summer carrion study of the baby pig *Sus Scrofa* linnaeus. *Ecology*
1804 **46**, 592–602 (1965).
1805
1806
1807 [50] Apprill, A., McNally, S., Parsons, R. & Weber, L. Minor revision to V4 region SSU
1808 rRNA 806R gene primer greatly increases detection of SAR11 bacterioplankton.
1809 *Aquatic Microbial Ecology* **75**, 129–137 (2015).
1810
1811
1812
1813 [51] Parada, A. E., Needham, D. M. & Fuhrman, J. A. Every base matters: assessing
1814 small subunit rRNA primers for marine microbiomes with mock communities,
1815 time series and global field samples. *Environmental Microbiology* **18**, 1403–14
1816 (2016).
1817
1818
1819
1820
1821 [52] Arkin, A. P. *et al.* KBase: The United States Department of Energy Systems
1822 Biology Knowledgebase. *Nature Biotechnology* **36**, 566–569 (2018).
1823
1824
1825 [53] Bolger, A. M., Lohse, M. & Usadel, B. Trimmomatic: a flexible trimmer for
1826 Illumina sequence data. *Bioinformatics* **30**, 2114–2120 (2014).
1827
1828
1829 [54] Bushnell, B. BBTools software package (2014).
1830
1831
1832 [55] Li, D., Liu, C.-M., Luo, R., Sadakane, K. & Lam, T.-W. MEGAHIT: an ultra-fast
1833 single-node solution for large and complex metagenomics assembly via succinct
1834 de Bruijn graph. *Bioinformatics* **31**, 1674–1676 (2015).
1835
1836
1837 [56] Hyatt, D. *et al.* Prodigal: prokaryotic gene recognition and translation initiation
1838 site identification. *BMC Bioinformatics* **11**, 119 (2010).
1839
1840

- [57] Cantalapiedra, C. P., Hernández-Plaza, A., Letunic, I., Bork, P. & Huerta-Cepas, J. eggNOG-mapper v2: functional annotation, orthology assignments, and domain prediction at the metagenomic scale. *Molecular Biology and Evolution* **38**, 5825–5829 (2021).
- [58] Buchfink, B., Reuter, K. & Drost, H.-G. Sensitive protein alignments at tree-of-life scale using DIAMOND. *Nature Methods* **18**, 366–368 (2021).
- [59] Robinson, M. D., McCarthy, D. J. & Smyth, G. K. edgeR: a Bioconductor package for differential expression analysis of digital gene expression data. *Bioinformatics* **26**, 139–140 (2010).
- [60] Smyth, G. K. in *limma: Linear Models for Microarray Data* (eds Gentleman, R., Carey, V. J., Huber, W., Irizarry, R. A. & Dudoit, S.) *Bioinformatics and Computational Biology Solutions Using R and Bioconductor* 397–420 (Springer New York, New York, NY, 2005).
- [61] Phipson, B. *et al.* Differential expression analysis (2020). URL <https://combine-australia.github.io/RNAseq-R/06-rnaseq-day1.html#References>.
- [62] Wickham, H. *ggplot2: Elegant Graphics for Data Analysis* (Springer-Verlag New York, 2016). URL <https://ggplot2.tidyverse.org>.
- [63] Oksanen, J. *et al.* *vegan: Community Ecology Package* (2024). URL <https://vegandevs.github.io/vegan/>.